metals

MDPI

Review

Innovations in Monitoring, Control and Design of Laser and Laser-Arc Hybrid Welding Processes

Zheng-Xiong Ma, Pei-Xin Cheng, Jie Ning *, Lin-Jie Zhang * and Suck-Joo Na

State Key Laboratory of Mechanical Behaviour for Materials, Xi'an Jiaotong University, Xi'an 710049, China; mzx1326910465@stu.xjtu.edu.cn (Z.-X.M.); chengpeixin@stu.xjtu.edu.cn (P.-X.C.); suckjoo.na@xjtu.edu.cn (S.-J.N.)
* Correspondence: j_ning@mail.xjtu.edu.cn (J.N.); zhanglinjie@mail.xjtu.edu.cn (L.-J.Z.); Tel.: +86-177-1956-7787 (J.N.); +86-181-0927-1105 (L.-J.Z.)

Abstract: With the rapid development of high power laser, laser welding has been widely used in many fields including manufacturing, metallurgy, automobile, biomedicine, electronics, aerospace etc. Because of its outstanding advantages, such as high energy density, small weld size, easy automation. Combining the two heat sources of laser and arc for welding can achieve excellent results due to the synergistic effect. Laser welding is a complicated physical and chemical metallurgical process, involving the laser beam and molten pool, keyholes and materials melting, evaporation and multiple physical process. Process monitoring and quality control are important content of research and development in the field of laser welding, which is the premise to obtain fine weld with high quality. Numerical simulation technology can describe many complex physical phenomena in welding process, which is very important to predict weld forming and quality and clarify the underline mechanism. In this paper, the research progress of process monitoring, quality control and autonomous intelligent design of laser and laser-arc hybrid welding based on numerical simulation were reviewed, and the research hotspots and development trends of laser welding in the future are predicted.

Keywords: laser welding; laser-arc hybrid welding; process monitoring; quality control; simulation

check for updates

Citation: Ma, Z.-X.; Cheng, P.-X.; Ning, J.; Zhang, L.-J.; Na, S.-J. Innovations in Monitoring, Control and Design of Laser and Laser-Arc Hybrid Welding Processes. *Metals* **2021**, *11*, 1910. https://doi.org/10.3390/met11121910

Academic Editor: Sergey N. Grigoriev

Received: 29 October 2021
Accepted: 23 November 2021
Published: 26 November 2021

Publisher's Note: MDPI stays neutral with regard to jurisdictional claims in published maps and institutional affiliations.

Copyright: © 2021 by the authors. Licensee MDPI, Basel, Switzerland. This article is an open access article distributed under the terms and conditions of the Creative Commons Attribution (CC BY) license (https://creativecommons.org/licenses/by/4.0/).

1. Introduction

With the requirement of industrial development for high efficiency, environmental protection and automation, the application of laser technology is rapidly popularized in many fields of manufacturing industry [1–6]. The rapid development of high-power fiber lasers provides a means for the fabrication of welding structures of the key materials in industry with high efficiency and precision in an open environment. On this basis, laser welding process has become one of the important aspects of laser application. Laser welding has the advantages of high energy density, small heating zone, large weld depth to width ratio, narrow heat affected zone, small deformation, high production efficiency, flexible control, etc. Compared with traditional fusion welding, such as arc welding, laser welding has higher welding speed and can produce high penetration, which significantly improve manufacturing productivity and reduce cost [7]. Compared with electron beam welding, laser welding also has the advantages of no vacuum chamber, in line with the development trend of low energy consumption, short process, high efficiency. In recent years, laser welding technology has been steadily improved, increasingly mature, which has obtained more and more attention [8–13]. Oliveira et al. [14] reported for the first time that the aged NiTi-20Zr high temperature shape memory alloy was laser welded. The results showed that the aged and welded NiTi-20Zr was mechanically loaded up to 500 MPa at room temperature and 200 °C, there was no fracture, and showed the same behavior as the reference base metal. The aged NiTi-20Zr alloy shows good Laser Weldability, which opens a new door for the use of these materials in drive-based applications, and this preliminary study shows a new possibility of using advanced laser bonding methods in

these alloys. Li et al. [15] studied the effects of linear, sinusoidal and cycloid scanning paths on flow dynamics and weld formation during laser welding of 5A06 aluminum alloy. The results show that when the scanning path is cycloid, it is helpful to reduce the formation of porosity due to its large heating area. Long et al. [16] studied the effect of the increase of ambient pressure on the penetration depth of laser welded molybdenum alloy. The results show that with the increase of ambient pressure, the energy required to form the penetration depth per unit length in the process of laser deep penetration welding increases. When the total energy of laser output is constant, the penetration depth of molybdenum alloy will decrease with the increase of ambient pressure. Because of its many advantages such as low heat input, small deformation, rapid cooling rate and high energy beam concentration, laser welding has good material adaptability. It can not only weld homogeneous materials but also suitable for welding dissimilar materials [17–21]. In production practice, dissimilar welding of different metals can reduce the weight of the structure and reduce the production cost. Moreover, the connection technology of heterogeneous materials plays an important role in the manufacture of complex structures, which has attracted the attention of many researchers [22–26]. Pereira et al. [27] studied laser welding of DP1000 steel and aluminum alloy 1050 H111 dissimilar metals. The results show that laser welding can successfully connect materials with very distinct material properties (thermal and mechanical). Cui et al. [28] used Dual-Beam Lasers with Side-by-Side Configuration to weld 1.5 mm thick dissimilar steel/aluminum. The results show that dual-beam laser welding with side-by-side configuration produces soundly welded steel/Al lapped joints free of welding defects. Murzin et al. [29] studied the pulsed laser welding of aluminum alloy AK4 and titanium alloy VT5-1, and obtained a uniform structure without voids, which indicates that the welded joint has high enough performance. Wallerstein et al. [30] reviewed the latest progress of laser welding between aluminum alloy and steel, and pointed out that connecting aluminum and steel is a challenging task, mainly because of the formation of brittle intermetallic compounds at the joint interface. Liedl et al. [31] studied the laser welding of 1mm aluminum alloy and steel dissimilar metals. The experimental research shows that by adjusting the laser power and welding speed, the ultra-thin diffusion zone with the minimum intermetallic layer thickness can be obtained, and then the weld without defects such as cracks and pores can be obtained. Wallerstein et al. [32] studied the optical fiber laser welding brazing of 6061-T6 aluminum alloy with a thickness of 1.6 mm and S235-JR structural steel with a thickness of 1.5 mm. The results show that the best AA6061 to S235 dissimilar joints can be obtained by combining AlSi5 welding wire with ALSi12 powder mixed in brazing flux.

However, the energy utilization of laser welding process largely depends on the laser absorption rate of the material. For example, the absorption of copper to infrared laser is less than 5%, leading to the low energy utilization rate and poor quality with pores, cracks and spatters [33–35]. In order to avoid the problems of single laser welding, laser-arc hybrid welding is proposed. Laser-arc hybrid welding technology is an efficient new welding method. It can give full play to the advantages of two welding heat sources, producing synergistic effect, obtaining good welding quality and production benefits, improving the bridging ability of groove gap and obtaining greater welding penetration [36–40]. Therefore, laser-arc hybrid welding has attracted more and more attention [41–44].

Laser welding (especially deep penetration laser welding) process involves many complex physical phenomena of material melting, strong evaporation, plasma, fresnel absorption, multiple reflection etc. As well as the dynamic equilibrium conditions for the stable existence of keyhole and the influence mechanism of various factors on the shape of molten pool. In addition to the complex physical phenomena of single laser welding, the interaction between the two heat sources of laser and arc intensifies the complexity of the laser-arc hybrid welding process. Therefore, in order to ensure the quality of laser welding, give full play to its advantages of high speed and efficiency, and speed up its application process, revealing the mechanism, predicting and controlling the welding process is very difficult and important. For a long time, scholars have been

trying to reveal the important mechanism behind the complex physical phenomena of laser welding process, such as the stability of keyhole, the flow dynamics behavior of molten pool, gas-liquid-solid multiphase coupling dynamics behavior and the generation mechanism of welding defects, so as to further improve the controllability of laser welding process. With the increasing requirements of automation and intelligence in modern industry and the increasing dependence of modern manufacturing environment on high-performance monitoring system, the monitoring and quality control of laser welding process has become an important content in the research and development of laser welding field [45–49]. Seam tracking, defect detection, weld forming quality monitoring of laser welding process can be realized by collect various signals of the welding process by using inductor, capacitor, sound waves, photoelectric, visual and other kinds of sensors and processed them by computer [50]. These signals can be fed to the computer at the same time to adjust the welding parameters, finally realizing the high quality of laser welding process automation [51–53]. In the process of laser welding, it is difficult to accurately and quantitatively characterize important information, such as laser shielding rate caused by plasma and nano metal particle jet flow, metal evaporation behavior and flow and heat transfer behavior of molten pool, while these information is very important and necessary for controlling of weld formation and quality prediction. Numerical simulation technology can describe numerous complex physical phenomena in the welding process, which is an effective research means in the field of welding [54–59].

The purpose of this work is the research progress of the monitoring and quality control of laser welding and laser-arc hybrid welding process as well as the intelligent design of welding process based on numerical simulation. The development of laser welding quality control is summarized from two aspects of laser welding quality control and numerical simulation of laser welding process. The laser welding quality control is mainly discussed from two aspects of welding signal monitoring and quality control technology. There are also other problems in this field, which are addressed by such comprehensive application of innovations. This paper systematically introduces and summarizes the research progress of laser and laser-arc hybrid welding process monitoring, quality control and independent intelligent design based on numerical simulation, and points out the existing problems, which is of guiding significance for the research of laser welding and laser arc-hybrid welding in the future. Finally, the research hotspots and development trends of laser welding and laser-arc hybrid welding are forecasted.

2. Signal Monitoring

2.1. Single Signal Monitoring

In the field of real-time monitoring, various sensors have shown promise in detecting weld states. These include acoustic emission, audible sound, infrared detectors, ultraviolet detectors, electromagnetic acoustic transducers, and polyvinylidene fluoride. In addition to ordinary monitoring sensors, some special technologies can be used, such as on-line coherent imaging [60], X-ray diffractometer [61] and Hanover analyzer [62]. From the current research, the detection of laser welding process signal mainly focuses on sound, light, electricity and heat [63–71].

Lee et al. [63] developed a visual sensor without auxiliary light source and preview distance and a suitable image processing technology to directly monitor the molten pool and find the weld seam, which can be applied for automatic seam tracking in pulsed laser edge welding. Compared with the traditional vision sensor for automatic welding seam tracking, this new developed vision sensor effectively reduces the tracking error and is suitable for micro-welding of small parts.

Eriksson et al. [64] proposed a specially developed type of streak photography that gather optical signal of single pixel lines. Wang et al. [72] used two high-speed cameras to capture the welding image of laser-arc hybrid welding, and then reconstructed the weld bottom penetration state through signal processing algorithm. Ghosal et al. [73] used artificial neural network to monitor the penetration depth of laser-arc hybrid weld-

ing of magnesium alloy. The results show that the prediction results are very accurate. Zhang et al. [66] have developed a multiple-optical-sensor system to better depict the welding process, and the correlation analysis and the results show the captured signals by the multiple optical signal system have high coupling relationship with each other.

Zhou et al. [67] studied the laser welding quality evaluation method based on two-dimensional array ultrasonic probe, which is used to inspect the weld joint, analyzing the effect of fusion state on A-scan echo amplitude, and C-scan image of internal contact surface is established. Figure 1 shows schematic diagram of detection by two-dimensional array ultrasonic probe. Testing results show that this method is simple and feasible, while the accuracy error is less than 0.05 mm and hence it could completely meet the requirements of engineering application.

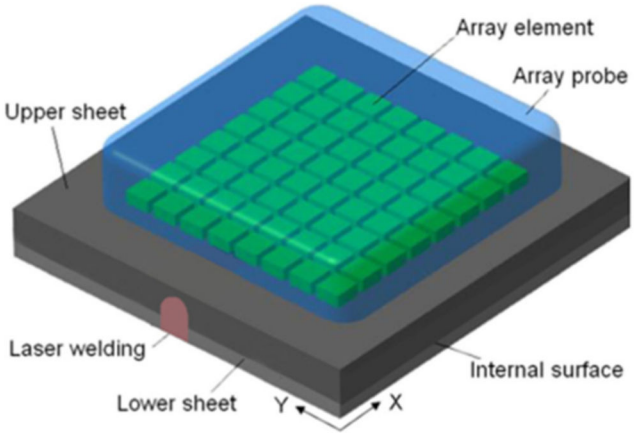

Figure 1. Schematic diagram of detection by two-dimensional array ultrasonic probe. Reprinted with permission from ref. [67]. Copyright 2021 Springer Nature.

In order to solve the problems of low tracking accuracy and high detection noise of weld deviation in high power narrow gap laser welding. Gao et al. [68] have proposed a method of seam tracking monitoring that employs a Sage-Husa adaptive Kalman filter (AKF)-embedded Elman neural network to detect the weld position. Firstly, a high speed near infrared imaging acquisition system is designed to collect the infrared images of molten pool and surrounding environment during laser welding. Then, the state and measurement equations for weld seam position were established based on an eigenvector derived from the weld seam position variable based on the collected near-infrared image sequence. Shao et al. [69] proposed a seam measurement method based on vision sensor to measure different wave length of laser for space weld seam of narrow butt joint in laser welding. The corresponding image process algorithm is proposed to extract the centerline of the red laser stripes as well as the seam feature.

Ancona et al. [70] have studied the CO_2 laser-induced plasma's optical signal emitted during welding of AISI 304 stainless steel and determined electron temperatures of the various chemical species that compose the plasma plume simultaneously by use of related emission lines. Na et al. [74] designed a low carbon steel pulse gas metal arc welding (GMAW) dynamic process monitoring system based on welding sound signal to identify different types of welding defects, especially cracks and pores.

2.2. Multi-Signal Coupling Monitoring

Real-time monitoring can avoid welding defects and improve welding quality. The monitoring results must be fed back to the control system immediately so that the control system can adjust the welding parameters in time, which means that the monitoring system needs to be accurate and efficient [75]. Because of the complexity of the laser welding, it is impossible to obtain the required useful information only by using a single sensor. From the perspective of current studies, multiple sensors are often used to sample multiple

detection signals at the same time, so as to improve the efficiency and accuracy through the mutual supplement of information between them. Some researches about sensor fusion have been investigated, which integrate the advantages of individual sensors to detect the signal [76–81].

Sun et al. [76] used the sensor fusion of infrared, ultraviolet (UV), audible sound (as) and acoustic emission (AE) sensors to evaluate the feasibility of real-time non-destructive weld penetration detection. The use of multiple sensors increased the reliability because the sensors tended to give complementary information. Zhang et al. [77] detected the welding defects based on deep learning with multiple optical sensors during disk laser welding of thick plates. They established the model between the in-process signals of the phenomena during high-power disk laser welding and the welding defects. This study provides a novel method to online detect the weld defects during high-power disk laser welding.

You et al. [78] conducted a study about data-driven analysis of multiple-input multiple-output (MIMO) laser welding process by integration of six advanced sensors. Figure 2 shows multiple sensing system for laser welding process. A multiple property measurement system is believed to be effective in specifying dynamic features of laser welding and providing accurate data for modeling of MIMO nonlinear process. This system consisted of six types of representative optical sensors including visible sensing photodiode, laser reflection sensing photodiode, spectrometer, visible sensing camera, auxiliary illumination sensing camera, and X-ray sensing camera. The characteristics variation of tendencies under different welding statuses were investigated. The feature spaces constructed for typical defects classification were demonstrated. Seven key sensing data (covering the optical, chemical, and physical aspects) was chosen for model output. Three controllable variables (including laser power, welding speed, defocus position) were considered as model input. This method can successfully represent the nonlinear energy input and nonlinear dynamic output of laser welding process. With the aid of the proposed multi-sensor system and designed nonlinear model, the relationship between the controllable variable and process status can be specified and used as reliable reference for advanced monitoring and intelligence control.

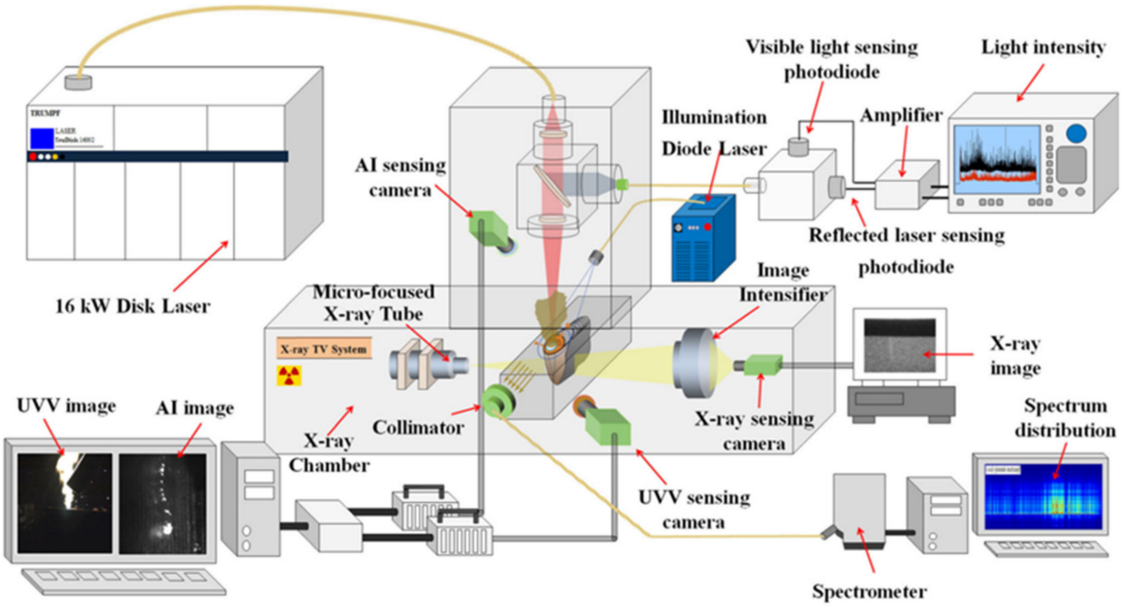

Figure 2. Multiple sensing system for laser welding process. Green zone indicated six sensors used in this research. Reprinted with permission from ref. [78]. Copyright 2021 Springer Nature.

3. Quality Control Technology

3.1. Process Optimization Control

The quality of the laser joint can be controlled effectively by traditional methods. The commonly used process optimization schemes include alloying, oscillating laser beam, changing the joint form, pulse laser, laser modulation and laser-arc heat source coupling.

Zhang et al. [79] investigated the effects of micro-alloying method on microstructure and properties of laser-welded Mo alloy joints, and Zr was selected as the additive material. They found that when Zr ring was added into the fusion zone, ZrO_2 was preferentially formed in the grain interior, which alleviated the segregation of MoO_2 and improved the tensile strength greatly. Zhou et al. [82] studied the welding of pure Cu and pure Mo dissimilar metals by single-mode laser welding, adding Ni as additive material. The results show that the tensile strength of the joint increases from 209.4 MPa to 288.5 MPa after adding nickel foil. Khodabakhshi et al. [80] have conducted the weldability of dissimilar lap joints between 2 mm thick sheets of AA6022 aluminum (bottom) and AZ31 magnesium alloys (upper) using a fiber laser with a wobbling scanner. Joint formation benefited from suppression of Al-Mg chemical reactions using a Ni-interlayer. Yang et al. [83] applied laser-metal inertia gas (MIG) hybrid welding to the welding of thick copper plates ($\geq$8 mm) for the first time, which provides a technical theoretical support for the laser-arc hybrid welding for high-reflective materials with large thickness. Zhang et al. [84] made a comparative study on the microstructure and properties of copper joint between MIG welding and laser-MIG hybrid welding. Compared with the double-sided metal inertia gas (DMIG) welded joint, the laser-metal inertia gas (HYBRID) welded joint exhibited narrower heat-affected zone (HAZ), finer grains in fusion zone (FZ) and HAZ, better electrical and thermal conductivities, and higher tensile strength. Guo et al. [85] compared the characteristics of high power fiber laser welding of thick section S700 high strength steel in the 1G and 2G positions. They found that welding 13 mm thick high-strength S700 steel plates in the 2G position can mitigate some of the common welding defects including undercut and sagging. Sun et al. [86] also conducted the fiber laser welding of thick AISI 304 plate in a horizontal (2G) butt joint configuration and contributed to a higher tensile strength.

Gao et al. [87] investigated the influence of pulse laser welding parameters on porosity and microstructure of Ti6Al4V welded joints. The results revealed that weld microstructure and porosity number in the pulsed laser welded Ti6Al4V joints are obviously correlated to overlapping factor and there is a critical overlapping factor above which porosities could be well avoided which offers a basis of reference for controlling the microstructure and porosity in titanium alloy. The number of porosities decreases with the increase in overlapping factor, and the welded joints are almost completely free of porosity when the overlapping factor is greater than 75%.

Ning et al. [34] selected AZ31 magnesium alloy to study the effect of power modulation on energy coupling efficiency in laser welding of highly-reflective materials. Figure 3 shows correlation between porosity number and overlapping factor. And the results indicated that the secret of improving energy coupling efficiency of laser welding process of highly-reflective materials through power modulation was the formation of a deep keyhole and its long life which pointed out the direction for the research of regulation measures and mechanism of the laser welding of highly-reflective materials.

3.2. Artificial Neural Network

Because of the complexity of the laser welding, it is impossible to obtain the required useful information only by using a single or multiple sensors. However, the information obtained by various sensors may be redundant or even contradictory. So, this requires the sensor "fusion" technology. In order to achieve this goal, neural network is a useful method. At the same time, neural network technology has a great potential in pattern classification and recognition. The neural network has a good learning ability, and the repeatability of laser welding process provides the neural network with learning conditions.

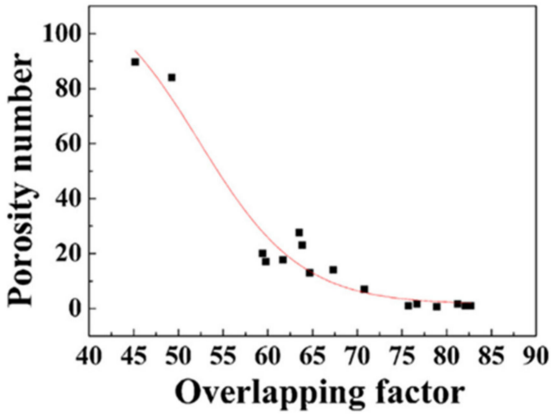

Figure 3. Correlation between porosity number and overlapping factor. Reprinted with permission from ref. [87]. Copyright 2021 Elsevier.

Sun et al. [88] suggested that incorporation of sensor fusion with neural networks will enable a highly robust and efficient system. Gao et al. [68] proposed a method of seam tracking monitoring which employs a Sage-Husa adaptive Kalman filter (AKF)-embedded Elman neural network to detect the weld position and solve the problems of low tracking accuracy and high detection noise of weld deviation in high power narrow gap laser welding. Zhang et al. [89] predicted the weld appearance with back propagation (BP) neural network improved by genetic algorithm during disk laser welding. BP neural network improved by genetic algorithm (GABP) is established to model the relation between welding appearance and the characteristics of the molten-pool-shadows. The work provides an effective way to predict the weld appearance and assess the welding quality in real-time. Zhang et al. [78] established a neural network model to make the learning judgment and simulated the possible defects in the welding process.

Ai et al. [56] proposed a defect-responsive optimization method for the fiber laser butt welding of dissimilar materials. The particle swarm optimization and back propagation neural network (PSO-BPNN), which has proved to be good modeling for no-linear problems, are utilized to establish the mathematical model. Johannes et al. [90] described a possible combination of recent reinforcement learning and deep learning algorithms and provided insights into the impact this combination may have on laser welding technology. It is the first demonstrated use of deep learning in laser welding and industrial production processes, see Figure 4. Algehyne1 et al. [91] used artificial neural network to simulate the dissimilar laser welding process of 304 stainless steel and copper, and used Bayesian rule back propagation training method to predict the temperature and melting rate in the dissimilar laser welding process of stainless steel and copper. The results show that the regression value has good accuracy in all cases.

3.3. Fuzzy Control

Kinsman et al. [92] studied a fuzzy logic control. The object of study is the number of pixels of holes and bright spots of plasma captured by the camera. The automatic adjustment of welding speed under fuzzy control was realized on the basis. The combination of fuzzy control and neural network is a new research method [93].

You et al. [94] introduced an innovative method to perform laser welding process monitoring and welding defect diagnosis. In addition, welded seam defects were defined according to the international standard by using the pattern recognition. Finally, a correlation model concerning optical features and geometrical parameters was established based on feedforward neural network (FNN), whereas the relation model concerning optical features and welded defects was built by support vector machine (SVM). This method provides an effective method to predict the geometrical parameters and detect welded defects by using optical features. Wang et al. [95] designed a fuzzy PI controller combined with fuzzy controller and proportional and integral controller to ensure the tracking perfor-

mance in the case of large offset and small offset. The welding experiments show that the proposed algorithm can track the path stably with high quality.

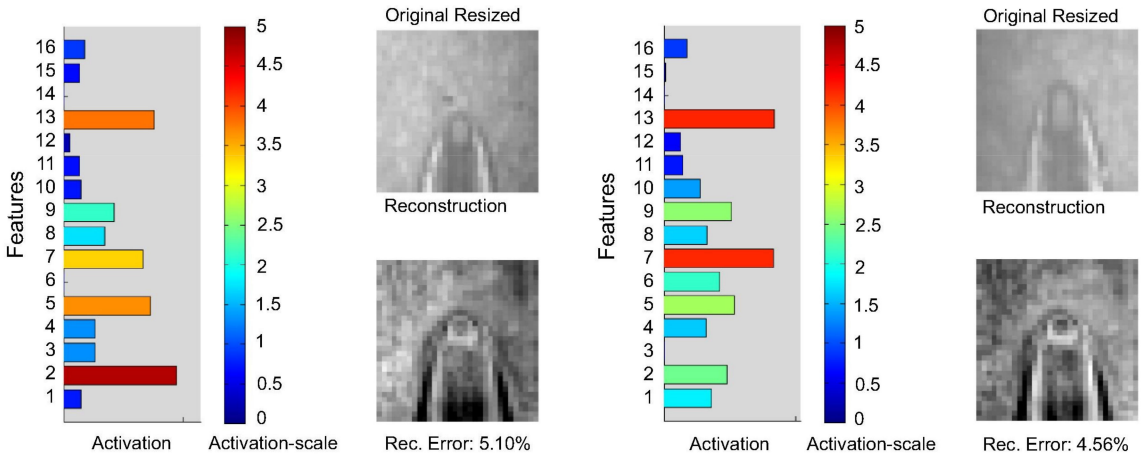

Figure 4. Neural network reaction to different inputs. The figure shows the original image (after preprocessing), the reconstruction, and the color-coded activations for two different processes. The error is the mean squared error (MSE) between the original image and the reconstruction. Reprinted with permission from ref. [90]. Copyright 2021 Elsevier.

4. Numerical Modeling

4.1. Mechanism

Kaplan et al. [96] proposed a model of deep penetration laser welding based on calculation of the keyhole profile. Pang et al. [97] conducted an efficient multiple time scale method for modeling the compressible vapor plume dynamics inside transient keyhole during fiber laser welding. The simulation results are shown in Figure 5. And two types of mathematical models are used to predict microstructure development in single-crystal nickel-base super alloys based on the typical physical phenomena occurring during laser-gas metal arc welding (GMA) hybrid welding. Ning et al. [98] conducted a numerical study of the effect of laser-arc distance on laser energy coupling in pulsed neodymium-doped yttrium aluminium garnet (Nd: YAG) laser/tungsten inert gas arc welding (TIG) hybrid welding. And the simulation technique considering the dynamic change of pore shape was applied to study the influence mechanism of heat source spacing and its physical mechanism for the first time.

Cho et al. [99] simulated and calculated the molten pool in laser -GMA hybrid welding process and an analysis was achieved using the Flow-3D commercial package. They found that due to the flow of the keyhole bottom, a vortex exists that mainly influences the shaping of the top bead. Trapped bubbles are observed in the pool because the keyhole collapse begins from the middle height of its depth. The penetration depth is strongly influenced by the laser.

Cosson et al. [100] proposed a numerical analysis of thermoplastic composites laser welding using ray a tracing method, while convergence of the model is defined during the calculation. Figure 6 is a multi-scale mesh representation of a 30% global volume fraction of the fiber packed reference cell. Using this computational method, it will be possible to study the influence of local fiber volume fraction variation without increasing the mesh preparation and computational time cost. The influence of the fiber architecture on the welding process can also be studied to determine the maximum substrate thickness that can be welded.

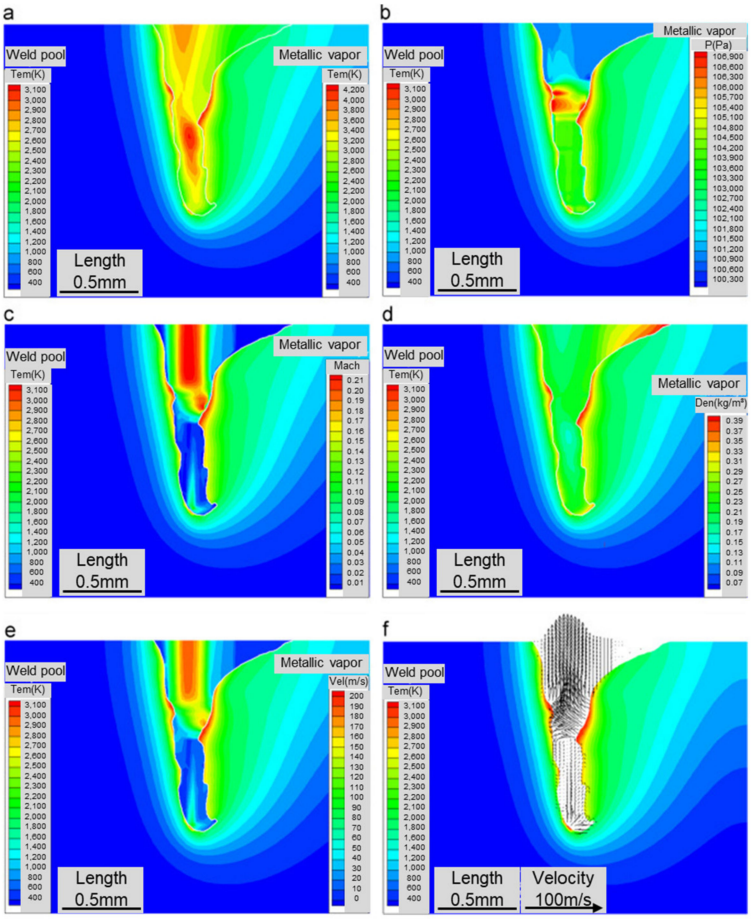

Figure 5. Distributions of temperature (**a**) pressure (**b**) Mach number (**c**) density (**d**) and velocity (**e**,**f**) of the metallic vapor inside keyhole at 15.006 ms (P = 1.5 kW, V = 3 m/min). Reprinted with permission from ref. [97]. Copyright 2021 Elsevier.

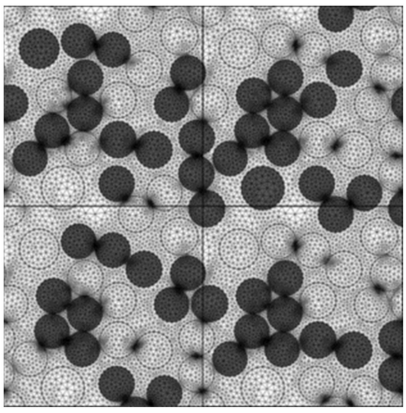

Figure 6. Multi-scale mesh representation for a 30% global volume fraction using fiber packed reference cells. In dark color: mesh elements considered as fibers, in light color mesh elements considered as polymer matrix. Reprinted with permission from ref. [100]. Copyright 2021 Elsevier.

4.2. Defects

Cho et al. [101] proposed a numerical study of alloying element distribution in CO_2 laser-GMA hybrid welding. All mathematical models for laser and arc welding are combined together without the interactions between the arc and laser heat sources. The laser model is modified to consider the optical geometry of the laser system; an additional conservation equation having the form of a general scalar advection equation is used for

simulating alloying element distributions. Zhang et al. [102] proposed a three dimensional laser deep penetration welding model in which volume of fluid (VOF) method was combined with a ray-tracing algorithm, to simulate the dynamic coupling between keyhole and molten pool in laser full penetration welding. Simulation results of the flow pattern of lower part in cross-sectional side views are shown in Figure 7. It can be seen from Figure 7a–e that volume of the melt in lower part continues to increase in the initial stage of laser full penetration welding.

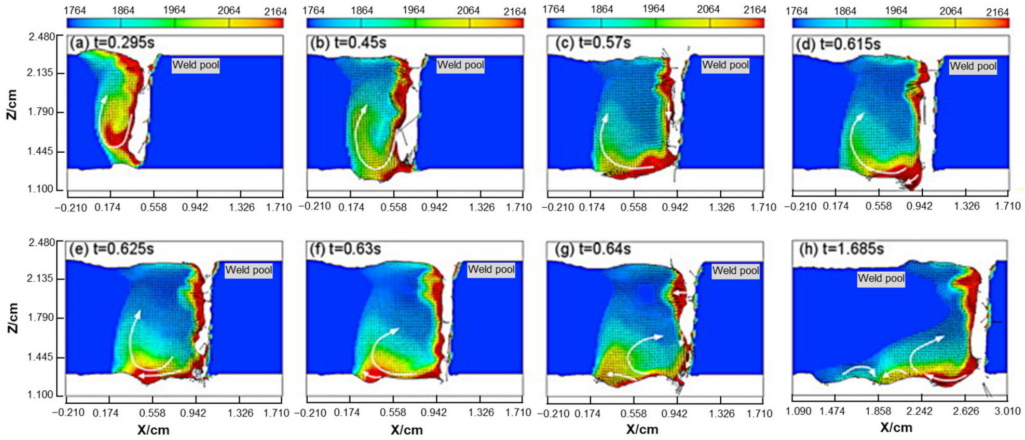

Figure 7. Simulation results of the flow pattern of lower part in cross-sectional side views. (**a**) t = 0.295 s, (**b**) t = 0.45 s. (**c**) t = 0.57 s, (**d**) t = 0.615 s, (**e**) t = 0.625 s, (**f**) t = 0.63 s, (**g**) t = 0.64 s, (**h**) t = 1.685 s. Reprinted with permission from ref. [102]. Copyright 2021 Elsevier.

Pang et al. [103] proposed the dynamics of vapor plume in transient keyhole during laser welding of stainless steel: Local evaporation, plume swing and gas entrapment into porosity. The possible process of the ambient gas entrapment into a bubble (<0.2 ms) during laser welding is numerically visualized. This might provide us another point of view to suppress the porosity defects. Panwisawas et al. [104] studied the keyhole formation and thermal fluid flow-induced porosity during laser fusion welding in titanium alloys by experimental and modelling. They found that as this molten pool grows in its size and depth, it becomes fully penetrating through the thickness of the joint. Where the vaporization of material occurs, the recoil pressure from the vaporized metal introduces a force upon the liquid metal. This imparts a deformation upon the molten region, and hence creates the vapor filled keyhole.

4.3. Crystal Growth

Tan et al. [105] studied the multi-scale modeling of solidification and microstructure development in laser keyhole welding process for austenitic stainless steel. On the macro-scale, a multi-phase and multi-physics model is utilized to predict the thermal history of molten pool during solidification; on the meso-scale, a 3D Cellular automata model has been developed to predict the competitive grain growth; on the micro-scale, a numerical model integrating Cellular Automata and Phase Field methods has been utilized to simulate the dendrite growth. Based on the typical physical phenomena occurring during laser-GMA hybrid welding, Gao et al. [106] proposed two types of mathematical models to predict the microstructure development in single-crystal nickel-base super alloys. Wei et al. [107] studied the crystal growth during keyhole mode laser welding. The temperature distribution and the transient thermal history of welds were combined with the grain growth simulation using a Monte Carlo approach in a computationally efficient manner. Gao et al. [108] carried out numerical analysis on the solidification temperature range to optimize the non-equilibrium solidification behavior of ternary Ni Cr Al single crystal nickel base superalloy during solidification with laser welding conditions (heat input or welding configuration). The experimental results well verified the theoretical prediction.

Badawy et al. [109] proposed a method combining classical molecular dynamics (MD) or finite element (FE) methods to develop metal laser welding model. The results show that the multi-scale model of metal laser welding is obtained by coupling continuous finite element method and discrete classical MD.

5. Conclusions and Prospect

In summary, laser welding has the characteristics of high precision, high efficiency and strong adaptability, and has the advantages of easy automatic control of parameters, good repeatability and reproducibility. It can improve the stability of product quality. Therefore, it has been widely used in many fields. Based on the industry's demand for automatic and intelligent welding, the research on the monitoring, quality control and monitoring-feedback-parameters adjust integrated control of laser welding process has attracted extensive attention. Various sensors such as inductance, capacitance, acoustic wave, photoelectric and vision are used to realize weld tracking, defect detection and weld forming quality monitoring according to different laser welding processes and requirements through artificial intelligence and computer processing methods; the welding process are adjusted through feedback control, so as to finally realize the automation and intelligence of laser welding process. Although scholars have conducted plenty of research, its application and promotion still face many bottlenecks to be broken through. The main reasons are as follows: on the one hand, the process window of laser welding is narrower than that of traditional arc welding, which is characterized by small weld pool size. Therefore, it is very sensitive to the fluctuation of assembly clearance and equipment state. It is easy to produce defects such as poor fusion, pores, cracks and splashes. On the other hand, the absorption rate of metallic material to laser directly affects the thermal efficiency and stability of welding process. In addition, the laser precision welding of ultra-thin and ultra-fine parts in the fields of electronics, communications and aviation, as well as the automatic intelligent welding of large thickness and large size parts in the fields of electric power, chemical industry and locomotives, have attracted wide attention.

Digital twin technology, which includes three main features of simulation model, big data and intelligence, is very suitable for the improvement of the design, control and operation of complex products and processing. The application of digital twin technology is expected to solve the dilemma that the research results of laser welding are slow to be applied in industrial field. However, the application of digital twin in laser processing is still in the exploratory stage. The digital twin of laser processing should consist of five modules: simulation model, sensing control model, statistical model, big data and machine learning module. How to realize the model establishment with high fidelity to study the physical mechanism of the interaction between laser and material, the heat transfer-flow-mass transfer behavior in laser welding pool of complex components, the thermal-metallurgy, thermal-mechanical coupling behavior in laser welding, and how to improve the efficiency of the model and realize the cooperation among multiple software and algorithm of coupling, developing the high quality, efficient and intelligent laser welding technology will be the research trend of laser welding technology in the future.

Author Contributions: Conceptualization, Z.-X.M. and J.N.; methodology, L.-J.Z.; software, J.N.; validation, Z.-X.M., J.N. and P.-X.C.; formal analysis, Z.-X.M.; investigation, J.N.; resources, J.N.; data curation, Z.-X.M.; writing—original draft preparation, Z.-X.M.; writing—review and editing, J.N.; visualization, S.-J.N.; supervision, L.-J.Z.; project administration, J.N.; funding acquisition, L.-J.Z. All authors have read and agreed to the published version of the manuscript.

Funding: This research was funded by National Natural Science Foundation of China, grant number 52005393 and China Postdoctoral Science Foundation, grant number 2020M683457.

Conflicts of Interest: The authors declare no conflict of interest.

References

1. Quintino, L.; Costa, A.; Miranda, R. Welding with high power fiber lasers—A preliminary study. *Mater. Des.* **2007**, *28*, 1231–1237. [CrossRef]
2. Nafisah, S.; Tukiran, Z.; Sheng, L.W.; Rohim, S.N.; Morsin, M. Laser Technology Applications in Critical Sectors: Military and Medical. *J. Electron. Volt. Appl.* **2021**, *2*, 2716–6074. [CrossRef]
3. Khan, B.A.; Litvinyuk, I.V.; Rybachuk, M. Femtosecond laser micromachining of diamond: Current research status, applications and challenges. *Carbon* **2021**, *179*, 209–226.
4. Wei, P.S.; Chuang, K.C.; Ku, J.S.; Debroy, T. Mechanisms of Spiking and Humping in Keyhole Welding. *IEEE Trans. Compon. Packag. Manuf. Technol.* **2012**, *2*, 383–394. [CrossRef]
5. Atabaki, M.M.; Yazdian, N.; Ma, J.; Kovacevic, R. High power laser welding of thick steel plates in a horizontal butt joint configuration. *Opt. Laser Technol.* **2016**, *83*, 1–12. [CrossRef]
6. Zhang, Y.; Li, F.; Liang, Z.; Ying, Y.; Lin, Q.; Wei, H. Correlation analysis of penetration based on keyhole and plasma plume in laser welding. *J. Mater. Process. Technol.* **2018**, *256*, 1–12. [CrossRef]
7. Patterson, T.; Hochanadel, J.; Sutton, S.; Panton, B.; Lippold, J. A review of high energy density beam processes for welding and additive manufacturing applications. *Weld. World* **2021**, *65*, 1235–1306. [CrossRef]
8. Jiang, M.; Jiang, N.; Chen, X.; Ma, S.; Chen, Y.; Chen, Y.; Lei, Z. Experimental and numerical investigation of single-pass laser welding of 20 mm-thick high-strength steel under reduced ambient pressure. *J. Mater. Res. Technol.* **2021**, *15*, 2317–2331. [CrossRef]
9. Huang, Y.; Shen, C.; Ji, X.; Li, F.; Hua, X. Correlation between gas-dynamic behaviour of a vapour plume and oscillation of keyhole size during laser welding of 5083 Al-alloy. *J. Mater. Process. Technol.* **2020**, *283*, 116721. [CrossRef]
10. Ning, J.; Zhang, L.J.; Wang, A.; Bai, Q.L.; Zhang, J.X. Effects of double-pass welding and extrusion on mechanical properties of fiber laser welded 1.5-mm thick T2 copper joints. *J. Mater. Process. Technol.* **2016**, *237*, 75–87. [CrossRef]
11. Heider, A.; Stritt, P.; Hess, A.; Weber, R.; Graf, T. Process Stabilization at welding Copper by Laser Power Modulation. *Phys. Procedia* **2011**, *12*, 81–87. [CrossRef]
12. Petring, D.; Goneghany, V.N. Parameter Dependencies of Copper Welding with Multi-kW Lasers at 1 Micron Wavelength. *Phys. Procedia* **2011**, *12*, 95–104. [CrossRef]
13. Zhang, L.L.; Zhang, L.J.; Long, J.; Sun, X.; Zhang, J.X.; Na, S.J. Enhanced mechanical performance of fusion zone in laser beam welding joint of molybdenum alloy due to solid carburizing. *Mater. Des.* **2019**, *181*, 107957. [CrossRef]
14. Oliveira, J.P.; Shen, J.; Escobar, J.D.; Salvador, C.; Benafan, O. Laser welding of H-phase strengthened Ni-rich NiTi-20Zr high-temperature shape memory alloy. *Mater. Des.* **2021**, *202*, 109533. [CrossRef]
15. Li, L.; Gong, J.; Xia, H.; Peng, G.; Hao, Y.; Meng, S.; Wang, J. Influence of scan paths on flow dynamics and weld formations during oscillating laser welding of 5A06 aluminum alloy. *J. Mater. Res. Technol.* **2020**, *11*, 19–32. [CrossRef]
16. Long, J.; Zhang, L.J.; Zhang, L.L.; Ning, J.; Yin, X.Q.; Zhang, J.X.; Na, S.J. Fiber laser spot welding of molybdenum alloy in a hyperbaric environment. *Opt. Express* **2020**, *28*, 7843–7857. [CrossRef]
17. Mousavi, S.; Sartangi, P.F. Experimental investigation of explosive welding of cp-titanium/AISI 304 stainless steel. *Mater. Des.* **2009**, *30*, 459–468. [CrossRef]
18. Howard, R.H.; Gallagher, R.C.; Field, K.G. Mechanical performance of neutron-irradiated dissimilar transition joints of aluminum alloy 6061-T6 and 304L stainless steel. *J. Nucl. Mater.* **2018**, *508*, 348–353. [CrossRef]
19. Yue, W.; Yan, C.; Wang, H.; Shi, S.; Hua, X.; Wu, Y. Investigation on microstructure and properties of dissimilar joint between SA553 and SUS304 made by laser welding with filler wire. *Mater. Des.* **2015**, *87*, 567–578.
20. Fazel-Najafabadi, M.; Kashani-Bozorg, S.F.; Zarei-Hanzaki, A. Dissimilar lap joining of 304 stainless steel to CP-Ti employing friction stir welding. *Mater. Des.* **2011**, *32*, 1824–1832. [CrossRef]
21. Anijdan, S.M.; Sabzi, M.; Ghobeiti-Hasab, M.; Roshan-Ghiyas, A. Optimization of spot welding process parameters in dissimilar joint of dual phase steel DP600 and AISI 304 stainless steel to achieve the highest level of shear-tensile strength. *Mater. Sci. Eng. A* **2018**, *726*, 120–125. [CrossRef]
22. Zhang, M.; Zhang, Z.; Tang, K.; Mao, C.; Hu, Y.; Chen, G. Analysis of mechanisms of underfill in full penetration laser welding of thick stainless steel with a 10 kW fiber laser. *Opt. Laser Technol.* **2018**, *98*, 97–105. [CrossRef]
23. Gao, S.L.; Li, Y.T.; Yang, L.Y.; Qiu, W.C. Microstructure and mechanical properties of laser-welded dissimilar DP780 and DP980 high-strength steel joints. *Mater. Sci. Eng. A* **2018**, *720*, 117–129. [CrossRef]
24. Pouranvari, M.; Abbasi, M. Dissimilar gas tungsten arc weld-brazing of Al/steel using Al-Si filler metal: Microstructure and strengthening mechanisms. *J. Alloys Compd.* **2018**, *749*, 121–127. [CrossRef]
25. Ebrahimian, A.; Kokabi, A.H. Friction stir soldering: A novel route to produce graphite-copper dissimilar joints. *Mater. Des.* **2017**, *116*, 599–608. [CrossRef]
26. Vidyarthy, R.S.; Kulkarni, A.; Dwivedi, D.K. Study of microstructure and mechanical property relationships of A-TIG welded P91-316L dissimilar steel joint. *Mater. Sci. Eng. A* **2017**, *695*, 249–257. [CrossRef]
27. Pereira, A.B.; Cabrinha, A.; Rocha, F.; Marques, P.; Fernandes, F.A.O.; Alves de Sousa, R.J. Dissimilar metals laser welding between DP1000 steel and aluminum alloy 1050. *Metals* **2019**, *9*, 102. [CrossRef]
28. Cui, L.; Chen, H.; Chen, B.; He, D. Welding of Dissimilar Steel/Al Joints Using Dual-Beam Lasers with Side-by-Side Configuration. *Metals* **2018**, *8*, 1017. [CrossRef]

29. Murzin, S.P.; Liedl, G. Laser welding of dissimilar metallic materials with use of diffractive optical elements. *Comput. Opt.* **2017**, *41*, 848–855. [CrossRef]
30. Wallerstein, D.; Salminen, A.; Lusquinos, F.; Comesana, R.; Garcia, J.D.; Rodriguez, A.R.; Badaoui, A.; Pou, J. Recent Developments in Laser Welding of Aluminum Alloys to Steel. *Metals* **2021**, *11*, 622. [CrossRef]
31. Liedl, G.; Vazquez, R.G.; Murzin, S.P. Joining of Aluminium Alloy and Steel by Laser Assisted Reactive Wetting. *Lasers Manuf. Mater. Process.* **2017**, *5*, 1–15. [CrossRef]
32. Wallerstein, D.; Lusquios, F.; Comesaa, R.; Val, J.D.; Pou, J. Dissimilar unbeveled butt joints of AA6061 to S235 structural steel by means of standard single beam fiber laser welding-brazing. *J. Mater. Process. Technol.* **2020**, *291*, 116994. [CrossRef]
33. Ning, J.; Zhang, L.; Zhang, L.L.; Long, J.; Na, S.J. Effects of power modulation on behaviours of molten pool and keyhole during laser-arc hybrid welding of pure copper. *Mater. Des.* **2020**, *194*, 108829. [CrossRef]
34. Ning, J.; Zhang, L.J.; Yin, X.Q.; Zhang, J.X.; Na, S.J. Mechanism study on the effects of power modulation on energy coupling efficiency in infrared laser welding of highly-reflective materials. *Mater. Des.* **2019**, *178*, 107871. [CrossRef]
35. Zhang, L.J.; Zhang, G.F.; Ning, J.; Zhang, X.J.; Zhang, J.X. Microstructure and properties of the laser butt welded 1.5-mm thick T2 copper joint achieved at high welding speed. *Mater. Des.* **2015**, *88*, 720–736. [CrossRef]
36. Zhang, M.; Shu, L.; Zhou, Q.; Jiang, P.; Gong, Z. On-line monitoring of penetration state in laser-arc hybrid welding based on keyhole and arc features. *J. Phys. Conf. Ser.* **2021**, *1884*, 012039. [CrossRef]
37. Liu, S.; Li, J.; Mi, G.; Wang, C.; Hu, X. Study on laser-MIG hybrid welding characteristics of A7N01-T6 aluminum alloy. *Int. J. Adv. Manuf. Technol.* **2016**, *87*, 1135–1144. [CrossRef]
38. Ogundimu, E.O.; Akinlabi, E.T.; Erinosho, M.F. Study on microstructure and mechanical properties of 304 stainless steel joints by TIG-MIG hybrid welding. *Surf. Rev. Lett.* **2018**, *25*, 1850042. [CrossRef]
39. Liu, T.; Yan, F.; Liu, S.; Li, R.; Wang, C.; Hu, X. Microstructure and mechanical properties of laser-arc hybrid welding joint of GH909 alloy. *Opt. Laser Technol.* **2016**, *80*, 56–66. [CrossRef]
40. He, C.; Huang, C.; Liu, Y.; Li, J.; Wang, Q. Effects of mechanical heterogeneity on the tensile and fatigue behaviours in a laser-arc hybrid welded aluminium alloy joint. *Mater. Des.* **2015**, *65*, 289–296. [CrossRef]
41. Qi, X.; Wang, X.; Di, H.; Shen, X.; Chen, L. Acicular ferrite nucleation mechanism in laser-MAG hybrid welds of X100 pipeline steel. *Mater. Lett.* **2021**, *304*, 130603. [CrossRef]
42. Wang, L.; Liu, Y.; Yang, C.; Gao, M. Study of porosity suppression in oscillating laser-MIG hybrid welding of AA6082 aluminum alloy. *J. Mater. Process. Technol.* **2021**, *292*, 117053. [CrossRef]
43. Wang, K.; Jiao, X.; Zhu, J.; Li, J.; Li, C. Research on the effect of weld groove on the quality and stability of laser-MAG hybrid welding in horizontal position. *Weld. World* **2021**, *65*, 1701–1709.
44. Bunaziv, I.; Akselsen, O.M.; Ren, X.; Nyhus, B.; Eriksson, M. Laser Beam and Laser-Arc Hybrid Welding of Aluminium Alloys. *Met. -Open Access Metall. J.* **2021**, *11*, 1150. [CrossRef]
45. Matsui, H.; Chiba, T.; Yamazaki, K. Detection and amplification of the molten pool natural oscillation in consumable electrode arc welding. *Weld. Int.* **2014**, *28*, 5–12. [CrossRef]
46. Ivan, B.; Jan, F.; Akselsen, O.M.; Kaplan, A. The penetration efficiency of thick plate laser-arc hybrid welding. *Int. J. Adv. Manuf. Technol.* **2018**, *97*, 2907–2919.
47. Guu, A.C.; Rokhlin, S.I. Arc weld process control using radiographic sensing. *Mater. Eval.* **1992**, *50*, 1344–1348.
48. Rsb, A.; Vjp, B. Process monitoring and internet of things feasibility for submerged arc welding: State of art. *Mater. Today Proc.* **2021**, *45*, 4441–4446.
49. Acherjee, B. Laser transmission welding of polymers—A review on welding parameters, quality attributes, process monitoring, and applications. *J. Manuf. Process.* **2021**, *64*, 421–443. [CrossRef]
50. You, D.Y.; Gao, X.D.; Katayama, S. Review of laser welding monitoring. *Sci. Technol. Weld. Join.* **2014**, *19*, 181–201. [CrossRef]
51. Luo, M.; Shin, Y.C. Vision-based weld pool boundary extraction and width measurement during keyhole fiber laser welding. *Opt. Lasers Eng.* **2015**, *64*, 59–70. [CrossRef]
52. Yu, J.; Lee, H.; Kim, D.Y.; Kang, M.; Hwang, I. Quality Assessment Method Based on a Spectrometer in Laser Beam Welding Process. *Met. -Open Access Metall. J.* **2020**, *10*, 839. [CrossRef]
53. He, Y.; Yu, Z.; Jian, L.; Ma, G.; Xu, Y. Fault correction of algorithm implementation for intelligentized robotic multipass welding process based on finite state machines. *Robot. Comput. -Integr. Manuf.* **2019**, *59*, 28–35. [CrossRef]
54. Nguyen, Q.Y.; Bagherzadeh, S.A.; Parsian, A.; Mohammad, A.; Karimipour, A. Nonlinear model identification of dissimilar laser joining of S.S 304 and ABS using the Hammerstein-Wiener method. *Optik* **2021**, *225*, 165649. [CrossRef]
55. Danielewski, H.; Skrzypczyk, A.; Tofil, S.; Rutkowski, S. Simulation of Laser Welding Dissimilar Low Carbon and Austenitic Steel Joint. *Open Eng.* **2020**, *10*, 491–498. [CrossRef]
56. Ai, Y.; Liu, X.; Huang, Y.; Yu, L. Numerical investigation of pore defect formation in the weld during high speed laser welding. *J. Laser Appl.* **2020**, *32*, 022066. [CrossRef]
57. Zhang, K.Z.; Lei, Z.L.; Chen, Y.B.; Yang, K.; Bao, Y.F. Microstructural evolution and numerical simulation of laser-welded Ti2AlNb joints under different heat inputs. *Rare Met.* **2021**, *40*, 2143–2153. [CrossRef]
58. Su, H.; Wu, C. Numerical Simulation for the Optimization of Polygonal Pin Profiles in Friction Stir Welding of Aluminum. *Acta Metall. Sin.* **2021**, *34*, 1065–1078. [CrossRef]

59. Halim, S.B.; Bannour, S.; Abderrazek, K.; Kriaa, W.; Autric, M. Numerical analysis of intermetallic compounds formed during laser welding of Aluminum-Magnesium dissimilar couple. *Therm. Sci. Eng. Prog.* **2021**, *22*, 100838. [CrossRef]
60. Pj, L.; Webster, L.G.; Wright, J.; Galbraith, C.M.; Kinross, A.W.; Vlack, V. Automatic laser welding and milling with in situ inline coherent imaging. *Opt. Lett.* **2014**, *39*, 6217–6220.
61. Kong, F.; Kovacevic, R. 3D finite element modeling of the thermally induced residual stress in the hybrid laser/arc welding of lap joint. *J. Mater. Process. Technol.* **2010**, *210*, 941–950. [CrossRef]
62. Zhang, F.; Liu, S.; Liu, F.; Zhang, H. Stability evaluation of laser-MAG hybrid welding process. *Opt. Laser Technol.* **2019**, *116*, 284–292. [CrossRef]
63. Lee, S.K.; Na, S.J. A study on automatic seam tracking in pulsed laser edge welding by using a vision sensor without an auxiliary light source. *J. Manuf. Syst.* **2002**, *21*, 302–315. [CrossRef]
64. Eriksson, I.; Gren, P.; Powell, J. New high-speed photography technique for observation of fluid flow in laser welding. *Opt. Eng.* **2010**, *49*, 100503. [CrossRef]
65. Eriksson, I.; Powell, J.; Kaplan, A.F.H. Measurements of fluid flow on keyhole front during laser welding. *Sci. Technol. Weld. Join.* **2011**, *16*, 636–641. [CrossRef]
66. Zhang, Y.X.; Zhang, N.F.; You, D.Y.; Gao, X.D.; Katayama, S.J. High-power disk laser welding statuses monitoring based on analyses of multiple-sensor signals. *J. Manuf. Process.* **2019**, *41*, 221–230. [CrossRef]
67. Zhou, G.; Xu, G.; Gu, X. Research on evaluating laser welding quality based on two-dimensional array ultrasonic probe. *Int. J. Adv. Manuf. Technol.* **2016**, *84*, 1717–1723. [CrossRef]
68. Gao, X.; You, D.; Katayama, S. Seam tracking monitoring based on adaptive Kalman filter embedded Elman neural network during high-power fiber laser welding. *IEEE Trans. Ind. Electron.* **2012**, *59*, 4315–4325. [CrossRef]
69. Shao, W.J.; Huang, Y.; Zhang, Y. A novel weld seam detection method for space weld seam of narrow butt joint in laser welding. *Opt. Laser Technol.* **2018**, *99*, 39–51. [CrossRef]
70. Ancona, A.; Spagnolo, V.; Lugara, P.M.; Ferrara, M. Optical sensor for real-time monitoring of CO_2 laser welding process. *Appl. Opt.* **2001**, *40*, 6019–6025. [CrossRef] [PubMed]
71. Wang, L.; Mohammadpour, M.; Yang, B.; Gao, X.; Kovacevic, R. Monitoring of keyhole entrance and molten pool with quality analysis during adjustable ring mode laser welding. *Appl. Opt.* **2020**, *59*, 1576–1584. [CrossRef]
72. Wang, L.X.; Gao, D.; Chen, Z.Q. Status analysis of keyhole bottom in laser-MAG hybrid welding process. *Opt. Express* **2018**, *26*, 347–355. [CrossRef] [PubMed]
73. Ghosal, S.; Chaki, S. Estimation and optimization of depth of penetration in hybrid CO_2 LASER-MIG welding using ANN-optimization hybrid model. *Int. J. Adv. Manuf. Technol.* **2010**, *47*, 1149–1157. [CrossRef]
74. Na, L.; Chen, S.J.; Chen, Q.H.; Tao, W.; Chen, S.B. Dynamic welding process monitoring based on microphone array technology. *J. Manuf. Process.* **2021**, *64*, 481–492. [CrossRef]
75. Fan, X.; Gao, X.; Liu, G.; Ma, N.; Zhang, Y. Research and prospect of welding monitoring technology based on machine vision. *Int. J. Adv. Manuf. Technol.* **2021**, *115*, 3365–3391. [CrossRef]
76. Sun, A.; Kannatey, E.A.; Gartner, M. Monitoring of laser weld penetration using sensor fusion. *J. Laser Appl.* **2002**, *14*, 114–121. [CrossRef]
77. Zhang, Y.; You, D.; Gao, X.; Zhang, N.; Gao, P.P. Welding defects detection based on deep learning with multiple optical sensors during disk laser welding of thick plates. *J. Manuf. Syst.* **2019**, *51*, 87–94. [CrossRef]
78. You, D.; Gao, X.; Katayama, S. Data-driven based analyzing and modeling of MIMO laser welding process by integration of six advanced sensors. *Int. J. Adv. Manuf. Technol.* **2015**, *82*, 1127–1139. [CrossRef]
79. Zhang, L.J.; Liu, J.Z.; Pei, J.Y.; Ning, J.; Zhang, L.L.; Long, J. Effects of power modulation, multipass remelting and Zr addition upon porosity defects in laser seal welding of end plug to thin-walled molybdenum alloy. *J. Manuf. Process.* **2019**, *41*, 197–207. [CrossRef]
80. Khodabakhshi, F.; Shah, L.H.; Gerlich, A.P. Dissimilar laser welding of an AA6022-AZ31 lap-joint by using ni-interlayer: Novel beam-wobbling technique, processing parameters, and metallurgical characterization. *Opt. Laser Technol.* **2019**, *112*, 349–362. [CrossRef]
81. You, D.; Gao, X.; Katayama, S. Multisensor fusion system for monitoring high-power disk laser welding using support vector machine. *IEEE Ind. Inf.* **2014**, *10*, 1285–1295.
82. Zhou, X.R.; Ning, J.; Na, S.J.; Zhang, L.J. Microstructures and properties of the dissimilar joint of pure molybdenum/T2 copper by single-mode laser welding. *Int. J. Refract. Met. Hard Mater.* **2021**, *101*, 105667. [CrossRef]
83. Yang, J.N.; Zhang, L.J.; Ning, J.; Bai, Q.L.; Yin, X.Q.; Zhang, J.X. Single pass laser-MIG hybrid welding of 8-mm thick pure copper (T2) without preheating: Microstructure and properties. *Appl. Therm. Eng.* **2017**, *126*, 867–883. [CrossRef]
84. Zhang, L.J.; Bai, Q.L.; Ning, J.; Wang, A.; Yang, J.N. A comparative study on the microstructure and properties of copper joint between MIG welding and laser-MIG hybrid welding. *Mater. Des.* **2016**, *110*, 35–50. [CrossRef]
85. Guo, W.; Liu, Q.; Francis, J.A.; Li, L. Comparison of laser welds in thick section S700 high-strength steel manufactured in flat (1G) and horizontal (2G) positions. *CIRP Ann. -Manuf. Technol.* **2015**, *64*, 197–200. [CrossRef]
86. Sun, J.; Feng, K.; Zhang, K.; Guo, B.; Jiang, E.; Nie, P.; Huang, J.; Li, Z. Fiber laser welding of thick AISI 304 plate in a horizontal (2G) butt joint configuration. *Mater. Des.* **2017**, *118*, 53–65. [CrossRef]

87. Gao, X.L.; Zhang, L.J.; Liu, J.; Zhang, J.X. Porosity and microstructure in pulsed Nd: YAG laser welded Ti6Al4V sheet. *J. Mater. Process. Technol.* **2014**, *214*, 1316–1325. [CrossRef]
88. Sun, A.; Kannatey, E.A.; Gartne, M. Sensor systems for real-time monitoring of laser weld quality. *J. Laser Appl.* **1999**, *11*, 153–168. [CrossRef]
89. Zhang, Y.; Gao, X.; Katayama, X.S. Weld appearance prediction with BP neural network improved by genetic algorithm during disk laser welding. *J. Manuf. Syst.* **2015**, *34*, 53–59. [CrossRef]
90. Johannes, G.; Pilarski, P.M.; Helfrich, G. Intelligent laser welding through representation, prediction, and control learning: An architecture with deep neural networks and reinforcement learning. *Mechatronics* **2015**, *34*, 1–11.
91. Algehyne, E.A.; Saeed, T.; Ibrahim, M.; Berrouk, A.S.; Chu, Y.M. Investigation of dissimilar laser welding of stainless steel 304 and copper using the artificial neural network model. *J. Laser Appl.* **2021**, *33*, 022010. [CrossRef]
92. Kinsman, G.; Duley, W. *Fuzzy Logic Control of CO_2 Laser Welding*; The International Society for Optical Engineering: Washington, DC, USA, 1994; Volume 93, pp. 160–167.
93. Chen, S.B.; Wu, L.; Wang, Q.L. Self-learning fuzzy neural networks and computer vision for control of pulsed GTAW. *Weld. J.* **1997**, *76*, 201–209.
94. You, D.; Gao, X.; Katayama, S. WPD-PCA-Based Laser Welding Process Monitoring and Defects Diagnosis by Using FNN and SVM. *IEEE Trans. Ind. Electron.* **2015**, *62*, 628–636. [CrossRef]
95. Wang, N.; Zhong, K.; Shi, X.; Zhang, X.; Zhang, L. Fuzzy-PI double-layer stability control of an online vision-based tracking system. *Intell. Serv. Robot.* **2021**, *14*, 187–197. [CrossRef]
96. Kaplan, A. A model of deep penetration laser welding based on calculation of the keyhole profile. *J. Phys. D-Appl. Phys.* **1994**, *27*, 1805–1814. [CrossRef]
97. Pang, S.Y.; Chen, X.; Li, W. Efficient multiple time scale method for modeling compressible vapor plume dynamics inside transient keyhole during fiber laser welding. *Opt. Laser Technol.* **2016**, *77*, 203–214. [CrossRef]
98. Ning, J.; Zhang, L.J.; Na, S.J. Numerical study of the effect of laser-arc distance on laser energy coupling in pulsed Nd: YAG laser/TIG hybrid welding. *Int. J. Adv. Manuf. Technol.* **2017**, *9127*, 1129–1143. [CrossRef]
99. Cho, J.H.; Na, S.J. Three-Dimensional Analysis of Molten Pool in GMA-Laser Hybrid Welding. *Weld. J.* **2009**, *88*, 35–43.
100. Cosson, B.; Deléglise, M.; Knapp, W. Numerical analysis of thermoplastic composites laser welding using ray tracing method. *Compos. Part B Eng.* **2015**, *68*, 85–91. [CrossRef]
101. Cho, W.I.; Na, S.J.; Cho, M.H.; Lee, J.S. Numerical study of alloying element distribution in CO2 laser-GMA hybrid welding. *Comput. Mater. Sci.* **2010**, *49*, 792–800. [CrossRef]
102. Zhang, L.J.; Zhang, J.X.; Gumenyuk, A.; Rethmeier, M.; Na, S.J. Numerical simulation of full penetration laser welding of thick steel plate with high power high brightness laser. *J. Mater. Process. Technol.* **2014**, *214*, 1710–1720. [CrossRef]
103. Pang, S.Y.; Chen, X.; Shao, X.Y. Dynamics of vapor plume in transient keyhole during laser welding of stainless steel: Local evaporation, plume swing and gas entrapment into porosity. *Opt. Lasers Eng.* **2016**, *82*, 28–40. [CrossRef]
104. Panwisawas, C.; Perumal, B.; Ward, R.M. Keyhole formation and thermal fluid flow-induced porosity during laser fusion welding in titanium alloys: Experimental and modelling. *Acta Mater.* **2017**, *126*, 251–263. [CrossRef]
105. Tan, W.D.; Yung, C. Multi-scale modeling of solidification and microstructure development in laser keyhole welding process for austenitic stainless steel. *Comput. Mater. Sci.* **2015**, *98*, 446–448. [CrossRef]
106. Gao, Z.; Ojo, O.A. Modeling analysis of hybrid laser-arc welding of single-crystal nickel-base superalloys. *Acta Mater.* **2012**, *60*, 3153–3167. [CrossRef]
107. Wei, H.L.; Elmer, J.W.; DebRoy, T. Crystal growth during keyhole mode laser welding. *Acta Mater.* **2017**, *133*, 10–20. [CrossRef]
108. Gao, Z.G. Numerical Analysis of Stray Grain Formation during Laser Welding Nickel-Based Single-Crystal Superalloy Part II: Multicomponent Dendrite Growth. *Mater. Sci. Forum* **2021**, *1033*, 31–39. [CrossRef]
109. Badawy, K.; Junaidi, S. A multiscale approach for modeling metal laser welding. *AIP Adv.* **2021**, *11*, 35308. [CrossRef]